

On Preheating in Higgs Inflation

Yuta Hamada^{a*}, Kiyoharu Kawana^{bc†} and Adam Scherlis^{d‡}

^a *Université de Paris, CNRS, Astroparticule et Cosmologie, F-75006 Paris, France,*

^b *Theory Center, High Energy Accelerator Research Organization (KEK),*

^c *Center for Theoretical Physics, Department of Physics and Astronomy,
Seoul National University, Seoul 08826, Korea,*

^d *Stanford Institute for Theoretical Physics, Department of Physics,
Stanford University, Stanford, CA 94305, United States*

February 10, 2021

Abstract

Recently, the problem of unitarity violation during the preheating stage of Higgs inflation with a large non-minimal coupling has been much discussed in the literature. We point out that this problem can be translated into a strong coupling problem for the dimensionless effective coupling, and that the existence of these problems is highly dependent on the choice of higher-dimensional operators because they can significantly change the background dynamics and the canonical normalization of the fluctuations around it. Correspondingly, the typical energy of particles produced during the first stage of preheating can remain comparable to or below the cutoff scale of the theory. As an example, we numerically calculate the particle production in the presence of a specific four-derivative operator of the Higgs field, and confirm the statement above. Our argument also applies to multi-field inflation with non-minimal couplings.

*E-mail: hamada(at)apc.in2p3.fr

†E-mail: kawana(at)post.kek.jp

‡E-mail: adam(at)scherlis.com

1 Introduction

Higgs inflation [1, 2, 3] with non-minimal gravitational coupling between the Ricci scalar and the Higgs is one of the simplest and most natural scenarios for cosmological inflation because it can be realized within the Standard Model (SM).¹ Higgs inflation is also connected to interesting phenomenology such as the production of primordial black holes [7, 8, 9, 10, 11]. In the case of a quartic potential i.e. $V(H) = \lambda_H(H^\dagger H)^2$, the quartic coupling λ_H and the non-minimal coupling ξ are constrained by the cosmic microwave background (CMB) normalization as $\lambda_H/\xi^2 \sim 10^{-9}$. Thus, as long as $\lambda_H = \mathcal{O}(10^{-3}-10^{-2})$, ξ has to have an unnaturally large value $\mathcal{O}(10^{3-4})$. Such a large value of ξ causes a few physical inconsistencies. For example, the unitarity of the model has been viewed with suspicion [12, 13, 14, 15, 16, 17] because the naive tree-level cutoff scale of the model is given by $\Lambda := M_{pl}/\xi$, and this is comparable with or smaller than other typical energy scales during the inflation. If this is the case, we cannot neglect higher-dimensional contributions such as $(H^\dagger H)^n/\Lambda^{2n-4}$ ($n \geq 3$) which is dominant over the quartic potential in the large-field region. Thus, the predictability or consistency of the model seems to be (strongly) UV-dependent. However, this problem was solved in [16] where it is argued that the cutoff scale Λ is a background-dependent quantity and can become sufficiently large relative to the relevant dynamical scales during the inflation.

However, large ξ (or small cutoff scale) is still problematic² when it comes to the preheating stage after inflation [20, 21, 22, 23, 24], see also [25, 26] for the earlier studies of (p)reheating after Higgs inflation. As discussed in [20], the background dynamics of the inflaton shows some spike-like behavior around its zero-crossings and can cause violent particle production of the Nambu-Goldstone (NG) modes of the inflaton or the longitudinal modes of the weak gauge boson. In particular, the typical energy scale of these produced particles is $\mathcal{O}(\sqrt{\lambda_H} M_{pl}) \gg \Lambda$, so the consistency of the theory during particle production is not clear. Therefore, even if it is consistent during inflation, the preheating dynamics still indicates the necessity of extending this model to a UV model which preserves unitarity.

In this paper, as a first step toward understanding the dynamics of these unitary models, we analyze the problem of unitarity during particle production after Higgs inflation by taking the effects of higher-dimensional operators into account. Among various higher-dimensional operators involving H , the most important ones are those that include ∂H because these problems originate in the behavior of ∂H around its (first) zero-crossing. We show that the issue of the strong coupling does not happen if operators like $(|\partial_\mu H|^2)^n/\Lambda^{4(n-1)}$ are present because they change the definition of the canonical field in terms of H around the zero-crossings. We study the dynamics of H and particle production after inflation in the

¹It is known that the SM Higgs potential can have a saddle point around the Planck scale when the top mass is around 171 GeV. However, we cannot use this fact to realize inflation purely within the SM because its inflationary predictions are inconsistent with cosmological observations [4, 5, 6]. Therefore, we need some extensions or mechanisms in order to regard the Higgs as an inflaton. Non-minimal coupling is one such possible extension.

²It is argued that this problem is absent in Palatini Higgs inflation [18, 19].

presence of a specific choice of higher-dimensional operator i.e. $(|\partial_\mu H|^2)^2/\Lambda^4$. We confirm that the strong coupling is absent in this case.

On the other hand, if an operator such as $(|H|^2)^2(|\partial_\mu H|^2)^2/\Lambda^8$ is added in addition to $(|\partial_\mu H|^2)^2/\Lambda^4$, we again face the strong coupling problem in general. Therefore, the fate of the perturbativity is highly UV-dependent, and the result changes depending on what types of higher dimensional operators are considered. From the low energy field theory point of view, there are infinitely many possibilities for the higher dimensional operators, and it is impossible to fix them.³ See [27] for the related discussion of the difference between prescription I and II in Higgs inflation. We claim that, among the infinitely many possibilities, there exist choices where the strong coupling does not arise, and the analysis of the preheating of Higgs inflation is self-consistent.

This paper is organized as follows. In Section 2, we briefly review inflation with a non-minimal coupling. In Section 3, we first show that the unitarity violation problem is translated into the strong coupling problem of the dimensionless effective couplings. Then, we show that the unitarity or strong coupling problem during the preheating stage is highly dependent on the choice of higher-dimensional operators in subsection 3.2. Next, we study particle production after inflation in the presence of a specific but important operator i.e. $|\partial_\mu H|^4/\Lambda^4$ in subsection 4. As is expected from the resolution of the unitarity problem, the existence of such a term significantly reduces the typical energy scale of produced particles, and we will see that this reduction is marginally consistent with the cutoff scale of the theory. The summary is presented in Section 5. In Appendix A, we briefly review the unitarity issue of Higgs inflation. The background dynamics in the conventional Higgs inflation is reviewed in Appendix B. The detail calculation of the particle production of the NG mode is presented in Appendix C.

2 Inflation with Non-minimal Coupling

In order to fix our notation, we first briefly review Higgs inflation [1]. See also [2] for the review. In the following discussion, the Higgs field in the Jordan frame is denoted by H , and the Hubble parameter in the Einstein frame is represented by \mathcal{H} to distinguish it from the Higgs field.

We start from the following action in the Jordan frame:

$$S = \int d^4x \sqrt{-g_J} \left(\frac{1}{2} M_{pl}^2 \Omega^2 R_J - g_J^{\mu\nu} D_\mu H (D_\nu H)^* - V_J(H) + \dots \right), \quad (1)$$

³The asymptotic scale/shift symmetry [16] does not constrain the operators relevant here.

where

$$V_J(H) = \lambda_H (|H|^2)^2, \quad \Omega^2 = 1 + 2\xi \frac{|H|^2}{M_{pl}^2}. \quad (2)$$

By performing the following redefinition of the metric field,

$$g_{\mu\nu} = \Omega^2 g_{J\mu\nu}, \quad (3)$$

we get

$$R_J = \Omega^2 \left[R_E + 3\Box \log \Omega^2 - \frac{3}{2} g^{\mu\nu} (\partial_\mu \log \Omega^2) (\partial_\nu \log \Omega^2) \right], \quad (4)$$

which leads to the action in the Einstein frame:

$$S = \int d^4x \sqrt{-g} \left(\frac{1}{2} M_{pl}^2 R - \frac{1}{\Omega^2} g^{\mu\nu} D_\mu H (D_\nu H)^* - \frac{3}{4} M_{pl}^2 (\partial_\mu \log \Omega^2)^2 - V(H) + \dots \right), \quad (5)$$

where

$$V(H) := \frac{V_J(H)}{\Omega^4} \quad (6)$$

is the potential in the Einstein frame. For the field value $|H|^2 \gg M_{pl}^2/\xi$, the kinetic term for the radial component of Higgs field is effectively given by the third term (the second term is neglected). Therefore, the canonically normalized field is

$$\chi := \sqrt{\frac{3}{2}} M_{pl} \log \Omega^2 \quad (\text{for } |H|^2 \gg M_{pl}^2/\xi). \quad (7)$$

Then, the action is

$$S = \int d^4x \sqrt{-g} \left[\frac{1}{2} M_{pl}^2 R - \frac{1}{\Omega^2} g^{\mu\nu} D_\mu H (D_\nu H)^* - \frac{1}{2} (\partial_\mu \chi)^2 - \frac{\lambda_H}{4} \frac{M_{pl}^4}{\xi^2} \left(1 - e^{-\sqrt{\frac{2}{3}} \frac{\chi}{M_{pl}}} \right)^2 + \dots \right], \quad (8)$$

from which we can see that the height of the potential is $\mathcal{O}(\lambda_H M_{pl}^4/\xi^2)$. Correspondingly, the Hubble scale is

$$\mathcal{H} = \frac{1}{M_{pl}} \sqrt{\frac{V}{3}} \sim \frac{1}{2} \sqrt{\frac{\lambda_H}{3}} \frac{M_{pl}}{\xi}. \quad (9)$$

The slow roll parameters are calculated as

$$\epsilon = \frac{M_{pl}^2}{2} \left(\frac{V'}{V} \right)^2 \simeq \frac{4}{3} \exp \left(-2\sqrt{\frac{2}{3}} \frac{\chi}{M_{pl}} \right), \quad \eta = M_{pl}^2 \frac{V''}{V} \simeq -\frac{4}{3} \exp \left(-\sqrt{\frac{2}{3}} \frac{\chi}{M_{pl}} \right), \quad (10)$$

where the prime represents the derivative with respect to χ . In addition, we also have a relation between the e-folding number N and ϵ, η :

$$N = \int dtH \simeq \frac{1}{M_{pl}^2} \int d\varphi \frac{V}{V'} \simeq \frac{\sqrt{3}}{2\epsilon^{1/2}} \Rightarrow \epsilon = \frac{3}{4N^2}, \quad \eta = -\frac{1}{N}. \quad (11)$$

Note that λ_H and ξ are not completely independent parameters because they are constrained by the CMB normalization [28]

$$A_s := \frac{V}{24\pi^2 \epsilon M_{pl}^4} \Big|_{k=k_*} \simeq 2.2 \times 10^{-9}. \quad (12)$$

where $k_* \simeq 0.05 \text{Mpc}^{-1}$ is the pivot scale. By substituting Eq. (11) into Eq. (12), we obtain

$$\frac{\lambda_H}{\xi^2} \simeq 6.3 \times \left(\frac{50}{N}\right)^2 \times 10^{-10}. \quad (13)$$

The value of λ_H is typically $\mathcal{O}(10^{-2})$ for a smaller top quark mass which realizes a stable electroweak vacuum [29, 30, 31]. In this case, the corresponding value of the non-minimal coupling is $\xi = \mathcal{O}(10^{3-4})$. If λ_H is tuned to be small at inflationary energy scales,⁴ then ξ can be as small as $\mathcal{O}(10)$, which is known as the critical Higgs inflation scenario [36, 37, 38].

Throughout this paper, we consider the case $\xi = \mathcal{O}(10^{3-4})$ and leave the analysis of (p)reheating in critical Higgs inflation for future investigation.

3 Unitarity Issue at the Preheating Stage in Higgs Inflation

3.1 Strong coupling problem during preheating

Let us consider the dynamics after inflation. As mentioned in the Introduction and Appendix A, the unitarity of this model during inflation is maintained because the cutoff scale is field-dependent [12, 13, 15, 16, 17]. On the other hand, it is known that there is still a unitarity issue during the preheating stage [20, 21, 22, 23, 24]. Here, we discuss this problem from a different point of view than these references, in the context of the strong coupling of the Higgs field. This viewpoint makes it easier to understand the role of higher-dimensional operators in unitarizing the theory in the next subsection.

Our starting point is Eq. (5). If we ignore the gauge field, the action is

$$S = \int d^4x \sqrt{-g} \left(\frac{1}{2} M_{pl}^2 R - \frac{1}{\Omega^2} |\partial_\mu H|^2 - \frac{3}{\Omega^4} \frac{\xi^2}{M_{pl}^2} (\partial_\mu |H|^2)^2 - V(H) + \dots \right). \quad (14)$$

⁴There are several proposals for an underlying mechanism of this tuning [32, 33, 34, 35].

We would like to consider the zero-crossing of the Higgs field. As we will see, the typical momentum scale associated with this process is much larger than the Hubble scale, and we can safely regard the background geometry as flat. Moreover, we can take Ω^2 to be 1 because the Higgs field is close to the origin. This results in the simplified action

$$S = \int d^4x \sqrt{-g} \left[\frac{1}{2} M_{pl}^2 R - |\partial_\mu H|^2 - \frac{3\xi^2}{M_{pl}^2} (\partial_\mu |H|^2)^2 - V(H) + \dots \right]. \quad (15)$$

Let us parametrize H as

$$H = \frac{1}{\sqrt{2}} \begin{pmatrix} \phi_1 + i\phi_2 \\ \phi_3 + i\phi_4 \end{pmatrix}. \quad (16)$$

By using this parametrization, the third term in Eq. (15) contains the $\phi_i^2 (\partial\phi_j)^2$ terms. For $i \neq j$, this is understood as the interaction term while, for $i = j$, this term changes the canonical normalization of ϕ_i field. To discuss whether the system is suffering from a strong coupling problem, it is convenient to move to the canonically normalized frame of the Higgs fields.

Indeed, we can move to the canonical frame order-by-order in $|H|^2$, by redefining the Higgs fields as⁵

$$H \rightarrow H - \frac{2\xi^2}{M_{pl}^2} |H|^2 H + \frac{6\xi^4}{M_{pl}^4} (|H|^2)^2 H + \dots, \quad (17)$$

which leads to

$$S = \int d^4x \sqrt{-g} \left[\frac{1}{2} M_{pl}^2 R - |\partial_\mu H|^2 + \frac{\xi^2}{M_{pl}^2} \left\{ 4|\partial_\mu H|^2 |H|^2 - (\partial_\mu |H|^2)^2 \right\} + \frac{2\xi^4}{M_{pl}^4} \left\{ -4|\partial_\mu H|^2 (|H|^2)^2 + |H|^2 (\partial_\mu |H|^2)^2 \right\} - \tilde{V}(H) + \dots \right], \quad (18)$$

where

$$\tilde{V}(H) := V \left(H - \frac{2\xi^2}{M_{pl}^2} |H|^2 H + \frac{6\xi^4}{M_{pl}^4} (|H|^2)^2 H \right) = \lambda_H (|H|^2)^2 - 8\lambda_H \frac{\xi^2}{M_{pl}^2} (|H|^2)^3 + \dots. \quad (19)$$

We can see that the expressions in the curly brackets in Eq. (18) do not contain the term ϕ_i^4 and ϕ_i^6 with two derivatives, as expected. On the other hand, other terms cannot be removed by the field redefinition, and can cause strong couplings as we will show in the following.

⁵It is possible to do the redefinition exactly, but it is not necessary here.

Next, suppose that the inflaton component is ϕ_1 . Then, the third term in Eq. (18) provides effective mass terms for $\phi_{2,3,4}$,

$$\begin{aligned}\mathcal{L}_{\phi^2} &= \frac{\xi^2}{M_{pl}^2} \left\{ 4|\partial_\mu H|^2 |H|^2 - (\partial_\mu |H|^2)^2 \right\} \\ &= -\frac{\lambda_H M_{pl}^2}{10} \left(\frac{\dot{\phi}_1^2}{0.1\lambda_H M_{pl}^4/\xi^2} \right) (\phi_2^2 + \phi_3^2 + \phi_4^2) + \dots, \end{aligned} \quad (20)$$

where we focused on the region $\phi_1 \sim 0$, $\dot{\phi}_1^2 \sim 0.1\lambda_H M_{pl}^4/\xi^2$ corresponding to the first zero-crossing. See Appendix B for details. The fourth term in Eq. (18) induces the following effective four-field terms,

$$\begin{aligned}\mathcal{L}_{\phi^4} &= \frac{2\xi^4}{M_{pl}^4} \left\{ -4|\partial_\mu H|^2 (|H|^2)^2 + |H|^2 (\partial_\mu |H|^2)^2 \right\} \\ &= \frac{2\xi^4}{M_{pl}^4} \dot{\phi}_1^2 \left\{ 2(|H|^2)^2 - |H|^2 \phi_1^2 \right\} + \dots \\ &= \frac{\lambda_H \xi^2}{10} \left(\frac{\dot{\phi}_1^2}{0.1\lambda_H M_{pl}^4/\xi^2} \right) (\phi_1^2 + \phi_2^2 + \phi_3^2 + \phi_4^2) (\phi_2^2 + \phi_3^2 + \phi_4^2) + \dots \\ &=: -\frac{1}{4}\kappa\phi_1^2 (\phi_2^2 + \phi_3^2 + \phi_4^2) - \frac{1}{4!}\rho (\phi_2^4 + \phi_3^4 + \phi_4^4) + \dots, \end{aligned} \quad (21)$$

where

$$\kappa = -\frac{2\lambda_H \xi^2}{5} \left(\frac{\dot{\phi}_1^2}{0.1\lambda_H M_{pl}^4/\xi^2} \right), \quad \rho = -\frac{12\lambda_H \xi^2}{5} \left(\frac{\dot{\phi}_1^2}{0.1\lambda_H M_{pl}^4/\xi^2} \right). \quad (22)$$

One can see that if $\lambda_H \xi^2 \gg 1$, the effective ϕ^4 couplings are non-perturbative, and the controllability of the theory is lost.⁶ This coupling is perturbative as long as the condition

$$\lambda_H \xi^2 \lesssim 10\pi \left(\frac{\dot{\phi}_1^2}{0.1\lambda_H M_{pl}^4/\xi^2} \right)^{-1} \left(\frac{\kappa_{\max}}{4\pi} \right), \quad \frac{5}{3}\pi \left(\frac{\dot{\phi}_1^2}{0.1\lambda_H M_{pl}^4/\xi^2} \right)^{-1} \left(\frac{\rho_{\max}}{4\pi} \right) \quad (23)$$

is satisfied. Here, κ_{\max} and ρ_{\max} are the maximum allowable values of the couplings κ and ρ , whose exact values are subject to debate. Combined with Eq. (13), we have

$$\xi \lesssim 470 \sqrt{\frac{N}{50}} \left(\frac{\dot{\phi}_1^2}{0.1\lambda_H M_{pl}^4/\xi^2} \right)^{-\frac{1}{4}} \left(\frac{\kappa_{\max}}{4\pi} \right)^{\frac{1}{4}}, \quad 300 \sqrt{\frac{N}{50}} \left(\frac{\dot{\phi}_1^2}{0.1\lambda_H M_{pl}^4/\xi^2} \right)^{-\frac{1}{4}} \left(\frac{\rho_{\max}}{4\pi} \right)^{\frac{1}{4}}. \quad (24)$$

⁶For $\lambda_H \xi^2 \gg 1$, the perturbativity is broken when $\dot{\phi}_1^2 \gtrsim (M_{pl}/\xi)^4$. This is interpreted as the unitarity violation scale, see Eq. (26).

In terms of λ_H , the bound is

$$\lambda_H \lesssim 1.4 \times 10^{-4} \left(\frac{50}{N}\right) \left(\frac{\dot{\phi}_1^2}{0.1\lambda_H M_{pl}^4/\xi^2}\right)^{-\frac{1}{2}} \left(\frac{\kappa_{\max}}{4\pi}\right)^{\frac{1}{2}}, \quad 5.7 \times 10^{-5} \left(\frac{50}{N}\right) \left(\frac{\dot{\phi}_1^2}{0.1\lambda_H M_{pl}^4/\xi^2}\right)^{-\frac{1}{2}} \left(\frac{\rho_{\max}}{4\pi}\right)^{\frac{1}{2}}. \quad (25)$$

The bounds Eqs. (24)(25) are also applicable to multi-field inflation with non-minimal couplings. We can see that the perturbativity condition is not satisfied in the conventional Higgs inflation scenario [1] while the critical Higgs inflation scenario [36, 37, 38] does not suffer from this problem. Nevertheless, if one naively continues the calculation of particle production assuming that the tree level action is correct, one finds very efficient production of the NG modes or the longitudinal gauge boson [20, 21, 22, 23, 24].

The values obtained in Eq. (24) are roughly consistent with the value $\xi^2 \lesssim 5 \times 10^4$ in [24], where the bound was derived by requiring that the maximum excited wavenumber is less than the unitarity violation scale M_{pl}/ξ .

3.2 Effect of Higher Dimensional Operators

Per the discussion in the previous subsection, it is impossible to study the preheating dynamics from a low-energy point of view. However, in this subsection, we show that for some specific choices of the higher-dimensional operators, the strong coupling issue does not arise. As an example, let us consider

$$\frac{c}{\Lambda_J^4} (|\partial_\mu H|^2)^2, \quad \Lambda_J := \frac{M_{pl}\Omega}{\xi} \left(1 + c' \left(\frac{\xi}{M_{pl}\Omega}\right)^2 |H|^2\right) \sim \frac{M_{pl}}{\xi} \quad \text{for } |H|^2 \ll \frac{M_{pl}^2}{\xi^2} \quad (26)$$

where c and c' are the coefficients, and Λ_J is the cutoff scale in Jordan frame estimated in Ref. [16].⁷ Note that this operator multiplied by $\sqrt{-g}$ is invariant under the transformation $g_{\mu\nu} \rightarrow \Omega^{-2}g_{\mu\nu}$ and does not change in the Einstein frame. When the Higgs crosses zero, this operator gives the effective kinetic term for the Higgs as

$$-c \frac{\xi^4}{2M_{pl}^4} \dot{\phi}_1^2 |\partial_\mu H|^2, \quad (27)$$

where $\dot{\phi}_1^2$ is almost constant (of order given in Eq. (34)). Hence, for the canonically normalized field $\tilde{H} := \sqrt{c/2} \xi^2 |\dot{\phi}_1| H/M_{pl}^2$, the effective mass Eq. (20) becomes smaller, and the four point coupling Eq. (18) remains perturbative. We notice that Eq. (26) generates an additional contribution to the effective mass and coupling. By expanding Λ_J^{-4} as a function of $|H|^2$, we

⁷Compared with [16], we treat the coefficient c' as a free parameter.

obtain

$$\begin{aligned}\Delta\mathcal{L}_{\phi^2} &= -\sqrt{\frac{\lambda_H}{c}} \frac{c'}{\xi} M_{pl}^2 \frac{\dot{\phi}_1^2}{\sqrt{\frac{\lambda_H}{c} \frac{M_{pl}^4}{\xi^3}}} \sum_i \tilde{\phi}_i^2, \\ \Delta\mathcal{L}_{\phi^4} &= \frac{5c'^2}{2c} \left(\sum_i \tilde{\phi}_i^2 \right)^2,\end{aligned}\tag{28}$$

which are again perturbative for moderate values of c and c' . In this way, the problem of the strong coupling is avoided, and we can safely discuss the dynamics of the preheating.

More generally, we may consider the operators

$$c_n \left[\frac{1}{\Lambda_J^4} |\partial_\mu H|^2 \right]^n |\partial_\mu H|^2, \quad d_m \left[\frac{1}{\Lambda_J^4} |\partial_\mu H|^2 \right]^m (|H|^2)^2,\tag{29}$$

where the first operator reduces the effective coupling by changing the kinetic term while the second one leads to a large coupling. In order to avoid the problem of strong coupling, the condition $2n \geq m$ needs to be realized.⁸ A similar perturbative condition is required for the other terms in the SM lagrangian such as the Yukawa and gauge couplings, and the Higgs mass term as well.

From the low energy viewpoint, there are infinitely many choices of c_n, d_m . Computing these values is a purely UV question. Here we point out that, among infinitely many possibilities from the low energy viewpoint, there exist choices where the self-consistency of the preheating process of Higgs inflation is maintained.

One may think that an operator such as Eq. (26) is inevitably generated by loop corrections, and that the problem of unitarity violation would disappear thanks to the loop-induced higher derivative term. However, since the loop correction accompanies many other operators, we also leave this possibility for future investigation.

During the inflation, the operator (26) may not modify the classical dynamics of the Higgs field but may play the role to generate the quantum fluctuation of the Higgs field. It is interesting to study if there is any observable consequence such as non-Gaussianities.

4 Particle Production

In this subsection, we discuss particle production with a specific choice of the higher-dimensional operator i.e. Eq. (26). We first study the background dynamics of the inflaton ϕ_1 in the presence of Eq. (26). See Appendix B (and Ref. [20]) for a discussion of the dynamics without higher-dimensional operators. The existence of Eq. (26) weakens the spike-like behavior in the inflaton dynamics [20]. As a result, the amount of particle production and the typical energy scale of the produced particles are reduced.

⁸We assume that the coefficient of the $\dot{\phi}_1^{2n+2}$ term in the Hamiltonian is positive. For $n = 1$, this follows from causality, unitarity, and analyticity arguments in a broad class of the theory [39].

4.1 Background Dynamics with Higher Dimensional operator

In the presence of Eq. (26), the equation of motion of ϕ_1 is

$$\ddot{\phi}_1 \left[1 + \frac{3c}{\Lambda_J^4} \dot{\phi}_1^2 \left(\frac{d\phi_1}{d\chi} \right)^2 \right] + 3\mathcal{H}\dot{\phi}_1 \left[1 + \frac{c}{\Lambda_J^4} \dot{\phi}_1^2 \left(\frac{d\phi_1}{d\chi} \right)^2 \right] + \frac{d^2\chi}{d\phi_1^2} \frac{d\phi_1}{d\chi} \dot{\phi}_1^2 - 3 \left(\frac{d\phi_1}{d\chi} \right)^2 \frac{c \frac{\partial \Lambda_J}{\partial \phi_1}}{\Lambda_J^5} \dot{\phi}_1^4 + \left(\frac{d\phi_1}{d\chi} \right)^2 \frac{\partial V}{\partial \phi_1} = 0, \quad (30)$$

where χ is the canonically normalized field of ϕ_1 whose exact definition is given by Eq. (75) in Appendix B. Around the origin, by neglecting the Hubble friction term and putting $d\chi/d\phi_1 \sim 1$, $d^2\chi/d\phi_1^2 \sim 3\xi^2\phi_1/M_{pl}^2$, this equation approximately becomes

$$\ddot{\phi}_1 + \ddot{\phi}_1 \frac{3c}{\Lambda_J^4} \dot{\phi}_1^2 + 3\xi^2 \frac{\phi_1}{M_{pl}^2} \dot{\phi}_1^2 + \lambda_H \phi_1^3 \sim 0, \quad (31)$$

from which we can see that the typical time scale is $\mathcal{O}(M_{pl}/\xi)$ and ⁹

$$\frac{d^{2n}\phi_1}{dt^{2n}} = \mathcal{O} \left(\left(\frac{M_{pl}}{\xi} \right)^{2n} \phi_1 \right), \quad \frac{d^{2n+1}\phi_1}{dt^{2n+1}} = \mathcal{O} \left(\left(\frac{M_{pl}}{\xi} \right)^{2n} \dot{\phi}_1 \right), \quad \text{for } 0 \leq n \in \mathbb{Z}, \quad \phi_1 \ll \frac{M_{pl}}{\xi}. \quad (32)$$

Note that the effects of Hubble friction do not change this parametric estimate because $\mathcal{H} = \mathcal{O}(\sqrt{\lambda_H} M_{pl}/\xi)$. The value of $\dot{\phi}_1$ around the origin can be evaluated by energy conservation,

$$\frac{1}{2} \dot{\chi}^2 + V + \frac{c}{4\Lambda_J^4} \dot{\phi}_1^4 \sim \frac{\lambda_H M_{pl}^4}{4\xi^2}, \quad (33)$$

from which we obtain

$$|\dot{\phi}_1| \sim \frac{\lambda_H^{1/4}}{\xi^{3/2} c^{1/4}} M_{pl}^2 \sim \frac{1}{(c \lambda_H \xi^2)^{1/4}} M_{pl} \mathcal{H}. \quad (34)$$

From this equation, we see that the spike-like feature is weaker than in the conventional case i.e. Eq. (79) by a factor of $(c \lambda_H \xi^2)^{-1/4}$. If we consider the higher order c_n operators in Eq. (29) instead of the four derivative operator, the value of $|\dot{\phi}_1|$ becomes smaller. Specifically, the first operator in Eq. (29) leads to a $\dot{\phi}_1^{2n+2}/\Lambda_J^{4n}$ term in the Lagrangian. By equating this to the inflation energy, we have

$$\dot{\phi}_1 \sim (\lambda_H \xi^2)^{\frac{1}{2n+2}} \Lambda_J^2 \sim \left(\frac{\xi}{200} \right)^{\frac{2}{n+1}} \left(\frac{50}{N} \right)^{\frac{1}{n+1}} \Lambda_J^2, \quad (35)$$

⁹The second and third terms in Eq. (31) cancel each other when $\ddot{\phi} \sim -(M_{pl}/\xi)\dot{\phi}$. Higher derivative terms are determined by taking the derivative.

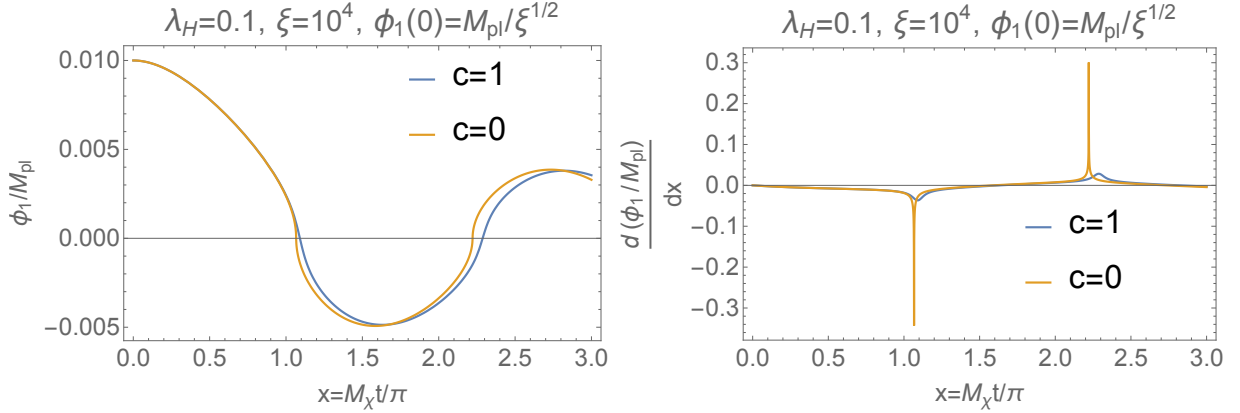


Figure 1: Upper left: The time evolution of ϕ_1 for $c = 0$ (orange) and $c = 1$ (blue). Upper right: The time evolution of $\dot{\phi}_1$ for $c = 0$ (orange) and $c = 1$ (blue). The parameter c' is taken to be 0. The unit of the time is Eq. (38).

where the CMB normalization condition Eq. (13) is used. This is a decreasing function of n for $\xi \gtrsim 200$.

Another important quantity for particle productions is the period for which the maximum value Eq. (34) is maintained. We denote the period by Δt_{sp} . The peak momentum of produced particles is given by the mass scale $m_{\text{sp}} = 1/\Delta t_{\text{sp}}$. The time scale Δt_{sp} is evaluated by using energy conservation. The energy density is dominated by the $3\xi^2\phi_1^2(\partial\phi_1)^2/M_{pl}^2$ term just after inflation. Then, the four-derivative term (26) becomes comparable to the $3\xi^2\phi_1^2(\partial\phi_1)^2/M_{pl}^2$ term at $\phi_1 = \tilde{\phi}$ where

$$\tilde{\phi}^2 \sim \frac{\lambda_H M_{pl}^2}{\xi}. \quad (36)$$

Here, we have used $\dot{\phi}_1^2 \sim \lambda_H M_{pl}^4/\xi^3$ right after inflation. (see Eq. (78) in Appendix B). The time scale Δt_{sp} is estimated as

$$\frac{1}{m_{\text{sp}}} = \Delta t_{\text{sp}} = \frac{\tilde{\phi}}{\dot{\phi}} \sim (c\lambda_H)^{1/4} \frac{\xi}{M_{pl}}, \quad (37)$$

which is longer than the typical time scale in Higgs inflation without the four derivative operator, $\Delta t_{\text{sp}}^0 \sim (\sqrt{\lambda_H} M_{pl})^{-1}$. (see Eq. (80) in Appendix B). The spike-like behavior of the inflaton becomes milder compared with the conventional case. It is expected that, if we add the higher order c_n operator in Eq. (29), the spike-like behavior becomes much milder.

In Fig. 1, we show our numerical calculations of ϕ_1 (left) and $\dot{\phi}_1$ (right), where blue and

orange lines correspond to $c = 1$ and 0 , respectively. Here, we define

$$M_\chi^2 = \lambda_H M_{pl}^2 / (3\xi^2) \simeq (1.45 \times 10^{-5} M_{pl})^2 \left(\frac{\lambda_H / \xi^2}{6.3 \times 10^{-10}} \right), \quad (38)$$

as a typical Higgs mass scale after inflation, and we choose $\lambda_H = 0.1$, $\xi = 10^4$. We see that the maximum value of $|\dot{\phi}_1|$ with $c = 1$ is suppressed by a factor of $\mathcal{O}(0.1)$ compared with that of $|\dot{\phi}_1|$ with $c = 0$. Furthermore, the maximum value of $|\dot{\phi}_1|$ with $c = 1$ is consistent with Eq. (34) within an order of magnitude.

The spike-like behavior of $\dot{\phi}_1(t)$ was first pointed out in [20], and this property plays an important role in particle production after Higgs inflation because the mass of particles typically depends on the derivatives of $\phi_1(t)$ when it is defined in the Jordan frame.

4.2 Brief Review of Particle Production

Let us consider particle production. Because the dynamics of ϕ_1 is significantly changed, the amount of produced particles also changes. In particular, as a consequence of Eq. (37), the typical energy scale of the produced particles is reduced by a factor of $\mathcal{O}(\xi^{-1})$ compared with the conventional case, i.e. m_{sp}^0 .

The time evolution of particle number density of a particle species φ is described by the Heisenberg equation [40, 41, 20]:

$$\varphi_k'' + \omega_k^2 \varphi_k = 0, \quad \omega_k^2 = k^2 + m_\varphi^2, \quad (39)$$

with the initial conditions

$$\varphi_k|_{\eta=0} = \frac{1}{\sqrt{2\omega_k}} \Big|_{\eta=0}, \quad \varphi_k'|_{\eta=0} = -i\omega_k \varphi_k|_{\eta=0}, \quad (40)$$

Here, a prime is the derivative with respect to the conformal time η , φ_k is the Fourier mode of the fluctuation φ , k is the absolute value of the comoving momentum of φ , and m_φ is the time-dependent mass. Equivalently, we can solve

$$\alpha_k'(\eta) = \frac{\omega_k'}{2\omega_k} e^{2i \int_0^\eta d\eta' \omega_k(\eta')} \beta_k(\eta), \quad \beta_k'(\eta) = \frac{\omega_k'}{2\omega_k} e^{-2i \int_0^\eta d\eta' \omega_k(\eta')} \alpha_k(\eta), \quad \alpha_k(0) = 1, \quad \beta_k(0) = 0, \quad (41)$$

where α and β are the Bogiliubov coefficients:

$$\varphi_k = \frac{1}{\sqrt{2\omega_k}} \left(\alpha_k e^{-i \int_0^\eta d\eta' \omega_k(\eta')} + \beta_k e^{i \int_0^\eta d\eta' \omega_k(\eta')} \right). \quad (42)$$

The particle number density n_φ per physical volume is defined by

$$n_\varphi(\eta) = \frac{1}{a^3} \int \frac{d^3k}{(2\pi)^3} f_\varphi(\eta, k), \quad f_\varphi(\eta, k) = \frac{1}{2\omega_k} (|\varphi_k'|^2 + \omega_k^2 |\varphi_k|^2) - \frac{1}{2} = |\beta_k|^2, \quad (43)$$

from which we define the energy density ρ_φ per physical volume as

$$\rho_\varphi(\eta) = \frac{1}{a^4} \int_0^\infty d(\log k) \tilde{\rho}_\varphi, \quad \tilde{\rho}_\varphi = \frac{k^3 \omega_k}{2\pi^2} f_\varphi. \quad (44)$$

In the following, we numerically study particle production in the following two cases:

- The inflaton is the Higgs field of a global $U(1)$ symmetry. We consider the production of the massless NG boson.
- The inflaton is the Higgs field of a $U(1)$ gauge symmetry. We consider the production of the longitudinal mode of the gauge boson.

The second one is close to the Higgs inflation case, and is of primary interest. On the other hand, the first one is not directly related to Higgs inflation. However, since a statement which is analogous to the equivalence theorem holds, we will find that the production of the NG boson and longitudinal gauge boson are similar for the high-momentum region.

As benchmark points, we study

$$\lambda_H = 10^{-3} \text{ and } 10^{-2}, \quad c = 1, \quad c' = 0, 0.1, \text{ and } 1. \quad (45)$$

The non-minimal coupling ξ is chosen in such a way that Eq. (13) is satisfied:

$$\xi \simeq \begin{cases} 1260 & \text{for } \lambda_H = 10^{-3} \\ 3980 & \text{for } \lambda_H = 10^{-2} \end{cases}. \quad (46)$$

In the model with the $U(1)$ gauge symmetry, we take the gauge coupling g to be 0.1.

4.3 Nambu-Goldstone Mode

Let us consider the production of the NG mode $\theta(x)$ of a complex scalar $\varphi_J(x) = r_J(x)e^{i\theta_J(x)/M_{pl}}/\sqrt{2}$ where $r_J(x)$ is regarded as an inflaton.

After the Weyl transformation $g_{\mu\nu} = \Omega^2 g_{J\mu\nu}$, the action is

$$S = \int d^4x \sqrt{-g} \left(-\frac{1}{2} g^{\mu\nu} \partial_\mu r \partial_\nu r - \frac{1}{2\Omega^2} g^{\mu\nu} \left(\frac{r_J}{M_{pl}} \right)^2 \partial_\mu \theta_J \partial_\nu \theta_J - V(r) + \frac{c}{\Lambda_J^4} (|\partial^\mu \varphi_J|^2)^2 \right), \quad (47)$$

where r is the canonically normalized field of r_J . From this action, we obtain the effective mass of the NG mode by defining the canonically normalized field $\theta(x)$. After the computation described in Appendix C, the frequency ω_k in Eq. (39) is given by

$$\omega_k^2 = k^2 + m_\theta^2, \quad m_\theta^2 = -\frac{F''}{F}, \quad F = \frac{ar_J}{\Omega M_{pl}} \sqrt{1 + \frac{c\Omega^2 r_J^2}{\Lambda_J^4}}. \quad (48)$$

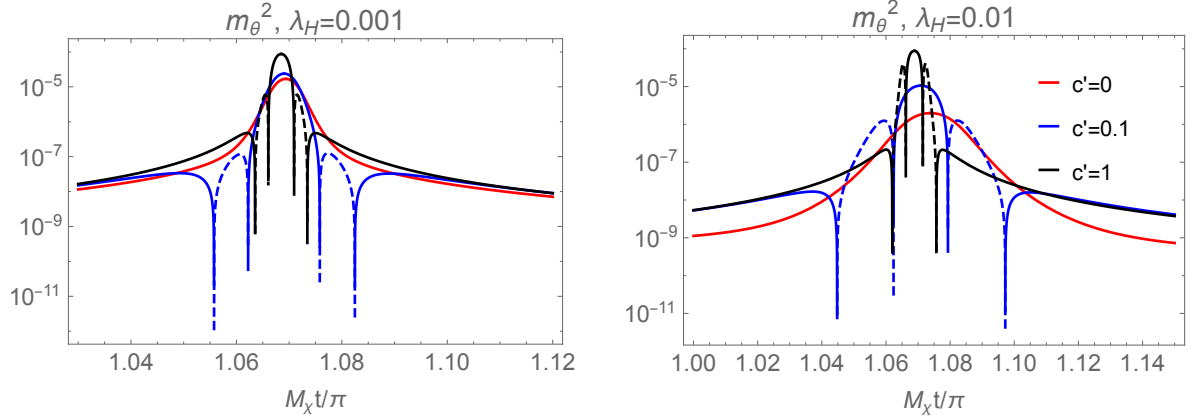


Figure 2: The plots of the effective mass squared of the NG mode. The solid and dashed lines correspond to the positive and negative signs, respectively. The left and right figures correspond to $\lambda_H = 10^{-3}$ and 10^{-2} , respectively. The unit of the time is Eq. (38).

In Fig. 2, we plot the effective mass of the NG mode around the first zero-crossing. The solid and dashed lines correspond to the positive and negative signs, respectively. We observe that, for $c' = 0.1$ and 1 , the mass square can be tachyonic. Moreover, the maximum value of m_θ^2 is larger than $c' = 0$ due to the contribution in Eq. (28). For these reasons, we expect that the particle production for $c' \neq 0$ is more efficient than $c' = 0$ case.

In Figs. 3 and 4, we show the numerical calculation of $f_\theta(k)$ and $\tilde{\rho}_\theta(k)$ after the first zero-crossing of ϕ_1 ($t = 1.5\pi/M_\chi$). The value of the cut off (damping) scale is consistent with our estimate Eq. (37) within an order of magnitude. The left and right figures correspond to $\lambda_H = 10^{-3}$ and 10^{-2} , respectively.

As for the total energy density ρ_θ , the numerical calculation is shown in Fig. 5. The vertical axis is normalized by the background energy density $3H^2 M_{pl}^2$. The gray vertical lines correspond to zero-crossings. The black horizon line corresponds to the value 0.1 , where the backreaction may become important. We find that, for $\lambda_H = 10^{-3}$, the backreaction becomes important within ten zero-crossings. On the other hand, for $\lambda_H = 10^{-2}$ and $c' = 0, 0.1$, the energy density ρ_θ is smaller than the background energy density for $t \leq 10\pi/M_\chi$. In these cases, we observe that ρ_θ is fitted by

$$\frac{\rho_\theta}{3H^2 M_{pl}^2} \simeq \begin{cases} 10^{-7} e^{0.5tM_\chi/\pi} & \text{for } (\lambda_H, c') = (10^{-2}, 0) \\ 2 \times 10^{-4} e^{0.3tM_\chi/\pi} & \text{for } (\lambda_H, c') = (10^{-2}, 0.1) \end{cases} . \quad (49)$$

If we can extrapolate this expression to larger t , we find that $\rho_\theta/(3H^2 M_{pl}^2)$ reaches 0.1 at the

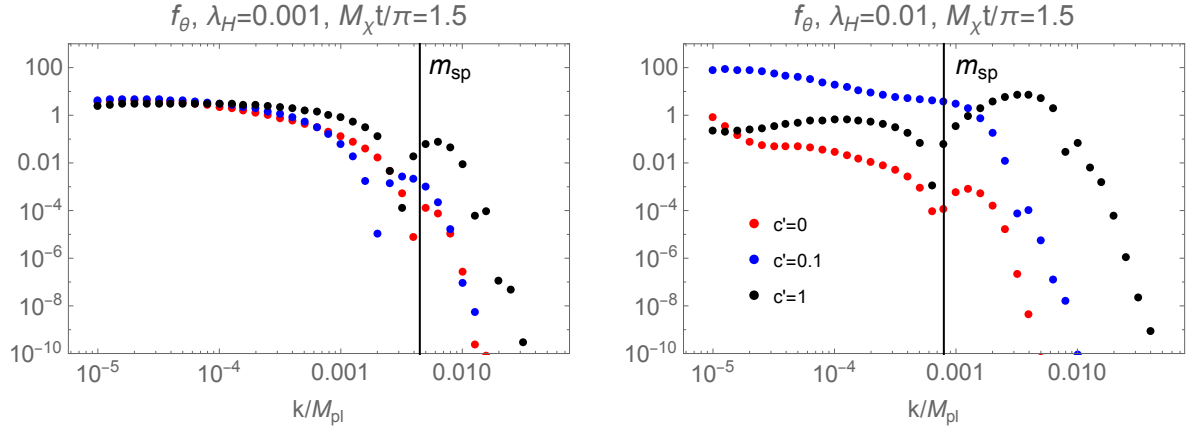


Figure 3: The plots of the occupation number of the NG mode θ , f_θ , after the first zero-crossing ($t = 1.5\pi/M_\chi$). The left and right figures correspond to $\lambda_H = 10^{-3}$ and 10^{-2} , respectively. The vertical line is the scale given in Eq. (37).

time

$$\frac{tM_\chi}{\pi} \simeq \begin{cases} 27 & \text{for } (\lambda_H, c') = (10^{-2}, 0) \\ 21 & \text{for } (\lambda_H, c') = (10^{-2}, 0.1) \end{cases} . \quad (50)$$

4.4 $U(1)$ Gauge Boson

In this subsection, we consider the Abelian Higgs model:

$$S = \int d^4x \sqrt{-g_J} \left(-\frac{1}{4} g_J^{\mu\alpha} g_J^{\nu\beta} F_{\mu\nu} F_{\alpha\beta} - g_J^{\mu\nu} (D_\mu \phi_J)^\dagger (D_\nu \phi_J) - V_J(|\phi_J|) + \frac{c}{\Lambda_J^4} \left[g_J^{\mu\nu} (D_\mu \phi_J)^\dagger (D_\nu \phi_J) \right]^2 \right). \quad (51)$$

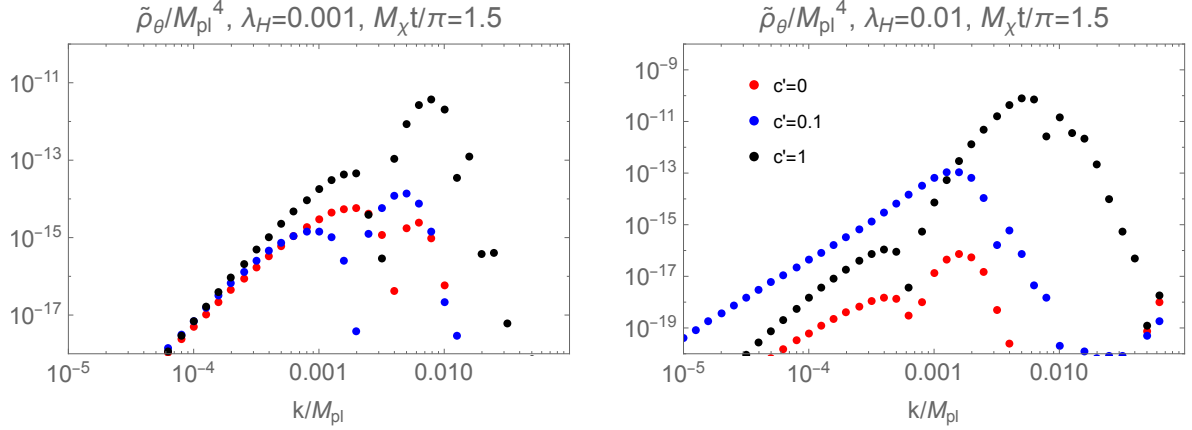


Figure 4: The plots of the energy density spectrum of the NG mode, $\tilde{\rho}_\theta$, after the first zero-crossing ($t = 1.5\pi/M_\chi$). The left and right figures correspond to $\lambda_H = 10^{-3}$ and 10^{-2} , respectively.

By moving to the Einstein frame and focusing on the kinetic part of the gauge boson, we have (See also Refs. [42, 20])

$$\begin{aligned}
S_A &:= \int d^4x \sqrt{-g_E} \left(-\frac{1}{4} g_E^{\mu\alpha} g_E^{\nu\beta} F_{\mu\nu} F_{\alpha\beta} - \frac{g^2}{2} r_J^2 \left(\frac{1}{\Omega^2} + \frac{c\dot{r}_J^2}{\Lambda_J^4} \right) g_E^{\mu\nu} A_\mu A_\nu \right) \\
&= \int d^4x a(t)^3 \left(\frac{1}{2a(t)^2} (\dot{A}_i - \partial_i A_0)^2 - \frac{1}{4a^4} \sum_{i,j=1}^3 (\partial_i A_j - \partial_j A_i)^2 - \frac{g^2}{2} r_J^2 \left(\frac{1}{\Omega^2} + \frac{c\dot{r}_J^2}{\Lambda_J^4} \right) (-A_0^2 + a(t)^{-2} \mathbf{A}^2) \right) \\
&= \int d\eta d^3x \left(\frac{1}{2} (A'_i - \partial_i A_\eta)^2 - \frac{1}{2} |\nabla \times \mathbf{A}|^2 - \frac{g^2 a^2}{2} r_J^2 \left(\frac{1}{\Omega^2} + \frac{c\dot{r}_J^2}{\Lambda_J^4} \right) (-A_\eta^2 + \mathbf{A}^2) \right) \\
&= \frac{1}{2} \int d\eta \int \frac{d^3k}{(2\pi)^3} \left((k^2 + m_A^2) |\tilde{A}_\eta|^2 - i\mathbf{k} \cdot \tilde{\mathbf{A}}' \tilde{A}_\eta + (\text{h.c.}) + \tilde{\mathbf{A}}'^2 - |\mathbf{k} \times \tilde{\mathbf{A}}|^2 - m_A^2 |\tilde{\mathbf{A}}|^2 \right) \\
&= \frac{1}{2} \int d\eta \int \frac{d^3k}{(2\pi)^3} \left((k^2 + m_A^2) \left| \tilde{A}_\eta - \frac{i\mathbf{k} \cdot \tilde{\mathbf{A}}'}{k^2 + m_A^2} \right|^2 - \frac{|\mathbf{k} \cdot \tilde{\mathbf{A}}'|^2}{k^2 + m_A^2} + |\tilde{\mathbf{A}}'|^2 - |\mathbf{k} \times \tilde{\mathbf{A}}|^2 - m_A^2 |\tilde{\mathbf{A}}|^2 \right), \tag{52}
\end{aligned}$$

where the unitary gauge is taken, $(\tilde{A}_\eta, \tilde{\mathbf{A}})$ represent the Fourier modes, r_J is the radial component of ϕ_J , g is a $U(1)$ coupling, and

$$m_A := \frac{g a r_J}{\Omega} \sqrt{1 + \frac{c\Omega^2 \dot{r}_J^2}{\Lambda_J^4}}. \tag{53}$$

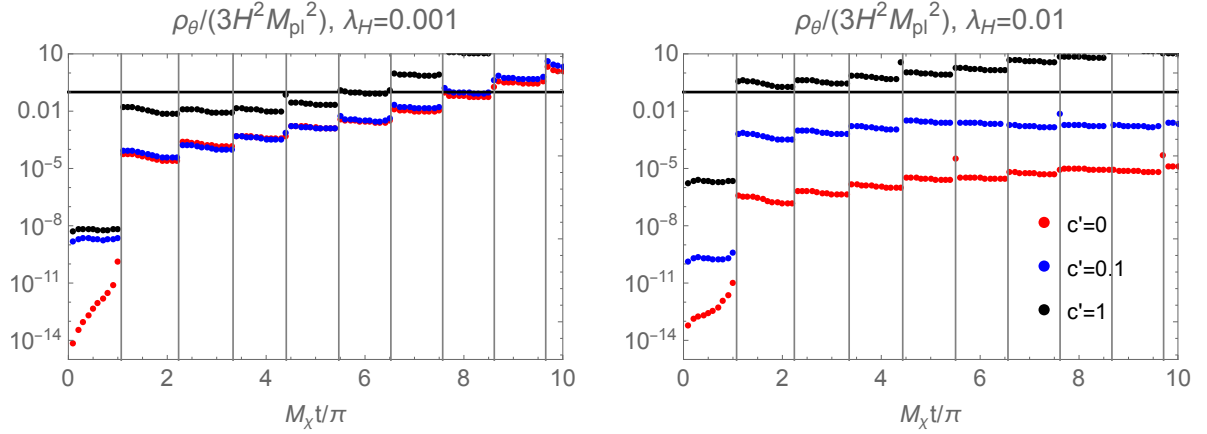


Figure 5: The plots of the energy density, ρ_θ , normalized by the background energy density as functions of t . The gray vertical lines correspond to zero-crossings. The black horizon line corresponds to the value 0.1, where the backreaction may become important. The left and right figures correspond to $\lambda_H = 10^{-3}$ and 10^{-2} , respectively. The unit of the time is Eq. (38).

After integrating \tilde{A}_η , we have

$$S_A \rightarrow S'_A = \frac{1}{2} \int d\eta \int \frac{d^3k}{(2\pi)^3} \left(|\tilde{A}'|^2 - \frac{|\mathbf{k} \cdot \tilde{\mathbf{A}}'|^2}{k^2 + m_A^2} - |\mathbf{k} \times \tilde{\mathbf{A}}|^2 - m_A^2 |\tilde{\mathbf{A}}|^2 \right). \quad (54)$$

Then, by decomposing $\tilde{\mathbf{A}}$ into the transverse and longitudinal modes as

$$\tilde{\mathbf{A}} := \tilde{\mathbf{A}}_T + \frac{\mathbf{k}}{|\mathbf{k}|} \tilde{A}_L, \quad \tilde{\mathbf{A}}_T \cdot \mathbf{k} = 0, \quad (55)$$

we obtain

$$\begin{aligned} S'_A &= \frac{1}{2} \int d\eta \int \frac{d^3k}{(2\pi)^3} \left(|\tilde{\mathbf{A}}'_T|^2 + |\tilde{A}'_L|^2 - \frac{k^2 |\tilde{A}'_L|^2}{k^2 + m_A^2} - |\mathbf{k} \times \tilde{\mathbf{A}}_T|^2 - m_A^2 (|\tilde{\mathbf{A}}_T|^2 + |\tilde{A}_L|^2) \right) \\ &= \frac{1}{2} \int d\eta \int \frac{d^3k}{(2\pi)^3} \left(|\tilde{\mathbf{A}}'_T|^2 - (k^2 + m_A^2) |\tilde{\mathbf{A}}_T|^2 + \frac{m_A^2 |\tilde{A}'_L|^2}{k^2 + m_A^2} - m_A^2 |\tilde{A}_L|^2 \right), \end{aligned} \quad (56)$$

from which we can see that the transverse component \mathbf{A}_T is already canonically normalized and its mass is given by m_A . Thus, it does not show any spike-like behavior and its particle production is similar to that of the broad resonance [25, 26].

On the other hand, the longitudinal component A_L is not canonically normalized, so we have to introduce a new field by

$$\tilde{\mathcal{A}}_L := \frac{m_A}{\sqrt{k^2 + m_A^2}} \tilde{A}_L. \quad (57)$$

Then, the action of \mathcal{A}_L becomes

$$\begin{aligned} & \frac{1}{2} \int d\eta \int \frac{d^3 k}{(2\pi)^3} \left(\left| \tilde{\mathcal{A}}'_L - \frac{m'_A}{m_A} \frac{k^2}{k^2 + m_A^2} \tilde{\mathcal{A}}_L \right|^2 - (k^2 + m_A^2) |\tilde{\mathcal{A}}_L|^2 \right) \\ &= \frac{1}{2} \int d\eta \int \frac{d^3 k}{(2\pi)^3} \left[\left| \tilde{\mathcal{A}}'_L \right|^2 - \left\{ k^2 + m_A^2 - \frac{d}{d\eta} \left(\frac{m'_A}{m_A} \frac{k^2}{k^2 + m_A^2} \right) - \left(\frac{m'_A}{m_A} \frac{k^2}{k^2 + m_A^2} \right)^2 \right\} |\tilde{\mathcal{A}}_L|^2 \right]. \end{aligned} \quad (58)$$

The particle production is computed by using Eq. (39) or (41) with

$$\omega_k^2(\eta) = k^2 + m_A^2 - \frac{d}{d\eta} \left(\frac{m'_A}{m_A} \frac{k^2}{k^2 + m_A^2} \right) - \left(\frac{m'_A}{m_A} \frac{k^2}{k^2 + m_A^2} \right)^2. \quad (59)$$

One can show that the effective mass obtained from this action coincides with that of the NG boson Eq.(48) for $k \gg m_A$ since m_A corresponds to F . As in the NG boson case, we find that it is possible to become $\omega_k^2 < 0$ for nonzero c' . As long as we focus on the main production mode $k \sim m_{\text{sp}}$, the mass difference is characterized by a small parameter

$$\varepsilon := \left(1 - \frac{k^2}{k^2 + m_A^2} \right) \Big|_{k=m_{\text{sp}}} \quad (60)$$

$$\sim 10^{-3} \times c^{1/2} \left(\frac{g}{0.1} \right)^2 \left(\frac{\lambda_H}{10^{-3}} \right)^2 \quad \text{for } r_J \lesssim \tilde{\phi} = (\lambda_H/\xi)^{1/2} M_{pl}, \quad (61)$$

where we have used Eqs. (13)(36). Thus, we expect that the qualitative behavior of particle production is similar between the NG boson and the longitudinal gauge boson for $k \gtrsim m_A$ except for the small corrections characterized by ε .

In Figs. 6 and 7, we show our numerical calculation of $f_{A_L}(k)$ and $\tilde{\rho}_{A_L}(k)$ after the first zero-crossing of ϕ_1 . Here, we choose $g = 0.1$. As in the NG boson case, we see that the damping scale is roughly given by m_{sp} in Eq. (37).

In Fig. 8, the total energy densities of the longitudinal gauge boson are plotted as functions of t . As in Fig. 5, the vertical axis is normalized by the background energy density $3H^2 M_{pl}^2$. The gray vertical lines correspond to zero-crossings, and the black horizon line corresponds to the value 0.1. We observe that the backreaction is important within the first ten zero-crossings except for $(\lambda_H, c') = (10^{-2}, 0)$ and $(10^{-2}, 0.1)$. In these cases, the energy densities are fitted by

$$\frac{\rho_{A_L}}{3H^2 M_{pl}^2} \simeq \begin{cases} 4 \times 10^{-5} e^{0.2tM_{\chi}/\pi} & \text{for } (\lambda_H, c') = (10^{-2}, 0) \\ 5 \times 10^{-4} e^{0.2tM_{\chi}/\pi} & \text{for } (\lambda_H, c') = (10^{-2}, 0.1) \end{cases}. \quad (62)$$

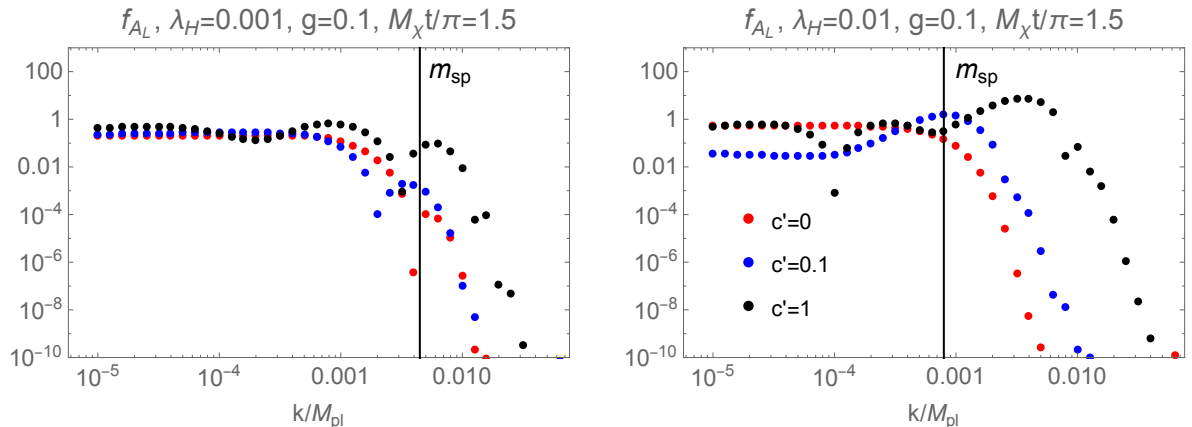


Figure 6: The plots of the occupation number of the longitudinal gauge boson, f_{A_L} , after the first zero-crossing ($t = 1.5\pi/M_\chi$). The left and right figures correspond to $\lambda_H = 10^{-3}$ and 10^{-2} , respectively. The $U(1)$ gauge coupling is taken to be $g = 0.1$. The vertical line is the scale given in Eq. (37).

If we can extrapolate this expression to a larger t , we find that the backreaction becomes important at the time

$$\frac{tM_\chi}{\pi} \simeq \begin{cases} 39 & \text{for } (\lambda_H, c') = (10^{-2}, 0) \\ 26 & \text{for } (\lambda_H, c') = (10^{-2}, 0.1) \end{cases} . \quad (63)$$

In a realistic situation, we notice that the longitudinal gauge boson decays into the light fermions in the SM. The energy density is expected to be smaller when we take into account the effect of the decay.

5 Summary

We have argued that the physics of Higgs inflation during the era of preheating is highly sensitive to the presence of higher-dimensional operators, and is therefore UV-dependent. In particular, we have shown that the operator $|\partial_\mu H|^4$ can dramatically alter the behavior of the Higgs dynamics during preheating and suppress the violent spike-like behavior that otherwise leads to high-energy particle production. This suppression maintains the consistency of the effective theory and avoids the unitarity problems associated with Higgs inflation.

As discussed above, there are many other higher-dimensional operators that can affect preheating. Further research is needed to determine which conditions and UV models allow unitarity to be preserved during Higgs inflation.

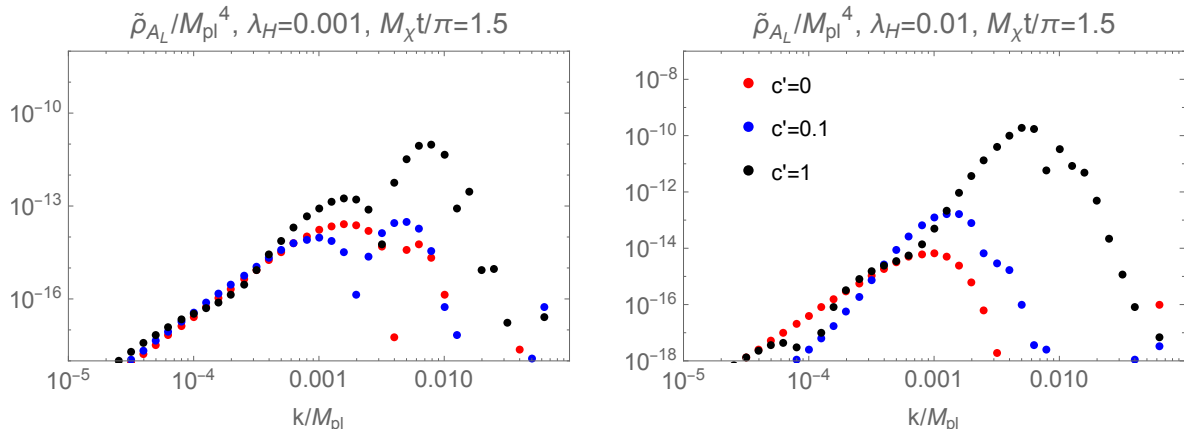


Figure 7: The plots of the energy density spectrum of the longitudinal gauge boson, $\tilde{\rho}_{A_L}$, after the first zero-crossing ($t = 1.5\pi/M_\chi$). The left and right figures correspond to $\lambda_H = 10^{-3}$ and 10^{-2} , respectively. The $U(1)$ gauge coupling is taken to be $g = 0.1$.

In order to have a better understanding of the preheating dynamics, it may be necessary to perform a lattice simulation that takes into account the non-linear effect (see e.g. Ref. [43] for a study of the preheating for the multifield inflation with non-minimal couplings). It is interesting to perform the lattice simulation with the higher dimensional operators.

Higgs inflation is a promising avenue for obtaining inflationary physics within the Standard Model. The UV-sensitivity of the unitarity problem allows us to constrain possible UV completions of this model, offering a valuable window into even higher-energy physics.

Acknowledgements

The work of YH is supported by the Advanced ERC grant SM-grav, No 669288. The work of KK is supported by the Grant-in-Aid for JSPS Research Fellow, Grant Number 17J03848. The work of AS is supported by DOE Grant DE-SC0012012, NSF Grant PHY-1720397, the Heising-Simons Foundation Grants 2015-037, and the Gordon and Betty Moore Foundation Grant GBMF7946. YH thanks the hospitality of the Kavli Institute for Theoretical Physics (supported by NSF PHY-1748958) where part of this work was carried out.

Appendix A Unitarity Issue in Higgs Inflation

In the Higgs inflation scenario with large non-minimal coupling $\xi \gg 1$, the naive tree-level cutoff scale $\Lambda = M_{pl}/\xi$ is comparable to or smaller than typical energy scales during inflation, e.g. $\mathcal{H} \sim \Lambda$, $\chi \sim M_{pl}$. However, in [16], it was argued that the cutoff scale Λ is actually a

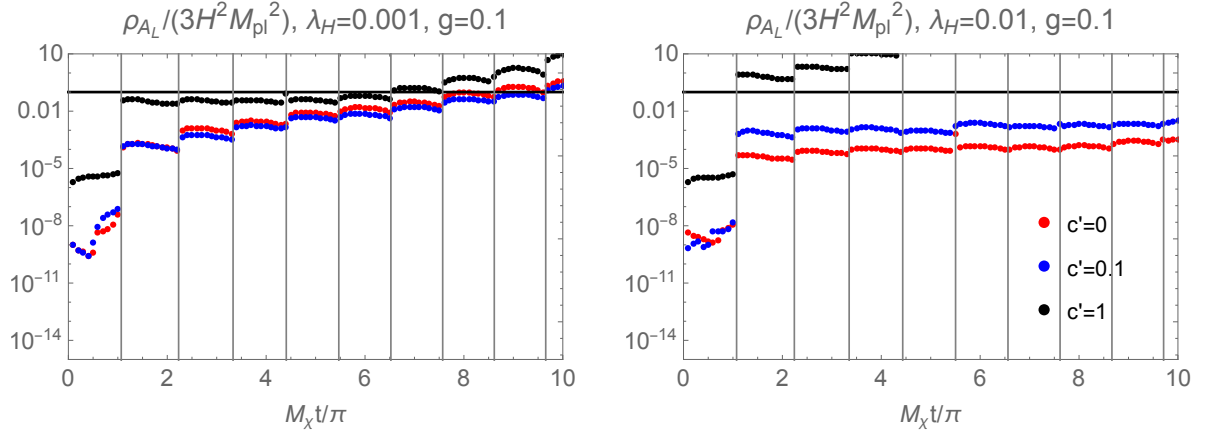


Figure 8: The plots of the energy density, ρ_{A_L} , normalized by the background energy density as functions of t . The gray vertical lines correspond to zero-crossings. The black horizon line corresponds to the value 0.1, where the backreaction may become important. The left and right figures correspond to $\lambda_H = 10^{-3}$ and 10^{-2} , respectively. The unit of the time is Eq. (38).

background-dependent quantity and remains sufficiently large compared with these relevant dynamical scales throughout the whole history of the universe. Here, we denote the Higgs in the Jordan frame as φ and choose the unitary gauge.

In the Jordan frame, by expanding the Higgs field and the metric around the backgrounds as $\varphi = \bar{\varphi} + \delta\varphi$, $g_{\mu\nu} = \bar{g}_{\mu\nu} + h_{\mu\nu}$ and redefining the canonically normalized fields ($\delta\hat{\varphi}, \hat{h}_{\mu\nu}$), we obtain various higher-dimensional operators. Among them, the leading one is the cubic Higgs-graviton interaction

$$\frac{\xi\sqrt{M_{pl}^2 + \xi\bar{\varphi}^2}}{M_{pl}^2 + (\xi + 6\xi^2)\bar{\varphi}^2}\delta\hat{\varphi}^2\Box\hat{h} := \frac{1}{\Lambda_J(\bar{\varphi})}\delta\hat{\varphi}^2\Box\hat{h} \quad (64)$$

where $\hat{h} = \bar{g}^{\mu\nu}\hat{h}_{\mu\nu}$ and $\Lambda_J(\bar{\varphi})$ is the cutoff scale in the Jordan frame. This behaves as

- For $\bar{\varphi} \ll M_{pl}/\xi$,

$$\Lambda_J(\bar{\varphi}) \simeq \frac{M_{pl}}{\xi} = \Lambda. \quad (65)$$

- For $M_{pl}/\xi \ll \bar{\varphi} \ll M_{pl}/\sqrt{\xi}$,

$$\Lambda \lesssim \Lambda_J(\varphi) \simeq \frac{6\xi\varphi_J^2}{M_{pl}} \ll 6M_{pl}. \quad (66)$$

- For $M_{pl}/\sqrt{\xi} \ll \bar{\varphi}$,

$$M_{pl} \lesssim \Lambda_J(\bar{\varphi}) \simeq 6\xi\bar{\varphi}. \quad (67)$$

Thus, because Higgs inflation occurs in the third region, $\Lambda_J(\bar{\varphi})$ is larger than the other dynamical scales \mathcal{H}, χ and consistent.

In the Einstein frame, the higher-dimensional operators only appear through the Higgs potential

$$V(\chi) = \frac{\lambda_H \varphi(\chi)^4}{4\Omega(\varphi(\chi))^4}, \quad (68)$$

where $\varphi(\chi)$ is a solution of

$$\frac{d\chi}{d\varphi} = \frac{1}{1 + \xi\varphi^2/M_{pl}^2} \sqrt{1 + \xi(1 + 6\xi) \frac{\varphi^2}{M_{pl}^2}}. \quad (69)$$

Then, we can repeat the same argument by expanding χ as $\chi = \bar{\chi} + \delta\chi$ and reading the cutoff scales from the expansion

$$V(\bar{\chi} + \delta\chi) = V(\bar{\chi}) + \sum_{n=1} \frac{1}{n! \Lambda_n^{n-4}} \delta\chi^n, \quad (70)$$

where

$$\Lambda_n := \left. \frac{d^n V(\chi)}{d\chi^n} \right|_{\chi=\bar{\chi}}^{-\frac{1}{n-4}}. \quad (71)$$

The results are

- For $\bar{\chi} \ll M_{pl}/\xi$,

$$\Lambda_n \sim \frac{M_{pl}}{\xi} \lambda_H^{-\frac{1}{n-4}}. \quad (72)$$

- For $M_{pl}/\xi \ll \bar{\chi} \ll M_{pl}$,

$$\Lambda_n \sim \frac{\xi \bar{\varphi}^2}{M_{pl}} \left(\frac{\xi^6 \bar{\varphi}^6}{\lambda_H M_{pl}^6} \right)^{\frac{1}{n-4}}, \quad (73)$$

- For $M_{pl}/\sqrt{\xi} \ll \bar{\chi}$,

$$\Lambda_n \sim M_{pl}. \quad (74)$$

These are consistent with Eqs. (65)(66)(67). See the paper [16] for a treatment including the quantum loop corrections.

Appendix B Inflaton Dynamics in Conventional Higgs Inflation

Here we discuss the background dynamics of the Higgs field after Higgs inflation in the conventional case. As the inflaton component, we choose ϕ_1 in Eq. (16). The canonically normalized real inflaton field χ is given by solving

$$\frac{d\chi}{d\phi_1} = \frac{1}{1 + \xi\phi_1^2/M_{pl}^2} \sqrt{1 + \xi(1 + 6\xi)\frac{\phi_1^2}{M_{pl}^2}}. \quad (75)$$

Then, its equation of motion is given by

$$\ddot{\chi} + 3\mathcal{H}\dot{\chi} = -\frac{\partial V}{\partial\chi} \simeq -M_\chi^2\chi, \quad \chi(0) \sim M_{pl}, \quad \dot{\chi}(0) \sim 0 \quad (76)$$

where $M_\chi^2 = \lambda_H M_{pl}^2/(3\xi^2) \sim \mathcal{H}$. If we neglect the friction term, the solution of this equation is just an oscillating solution $\chi(t) \sim M_{pl} \sin(M_\chi t)$. Therefore, there is no spike-like behavior for $\chi(t)$. On the other hand, the background dynamics of ϕ_1 have impulsive behavior when ϕ_1 passes the origin because of the change of the dominant kinetic term of ϕ_1 in Eq. (5). In fact, when $\phi_1 \gg M_{pl}/(\sqrt{6}\xi)$, the term containing $\partial \log \Omega(\phi_1)$ dominates, so the Lagrangian effectively becomes

$$\mathcal{L}_\chi \simeq 3\xi^2 \left(\frac{\phi_1}{M_{pl}} \right)^2 (\partial\phi_1)^2 - \frac{\lambda_H}{4} \phi_1^4 = 2\lambda_H \left(\frac{\phi_1}{M_\chi} \right)^2 \left(\frac{1}{2} (\partial\phi_1)^2 - \frac{1}{2} \left(\frac{M_\chi}{2} \right)^2 \phi_1^2 \right), \quad (77)$$

from which we can see that

$$|\dot{\phi}_1| \sim \frac{M_{pl}}{\sqrt{\xi}} \frac{M_\chi}{2} \quad (78)$$

at $\phi_1 \simeq M_p/\sqrt{\xi}$. After ϕ_1 drops below $M_{pl}/(\sqrt{6}\xi)$, the usual kinetic term starts to dominate. Therefore, from energy conservation, we have

$$\frac{1}{2} \dot{\phi}_1^2 \simeq V_I = \frac{\lambda M_{pl}^4}{4\xi^2} \quad \Rightarrow \quad \dot{\phi}_1 \simeq \sqrt{\frac{3}{2}} M_{pl} M_\chi, \quad (79)$$

which is larger than Eq. (78) by a factor of $\xi^{1/2}$. Thus, $\dot{\phi}_1(t)$ indicates spike-like behavior around the origin. The corresponding time scale $\Delta t_{\text{sp}}^0 := 1/m_{\text{sp}}^0$ is given by

$$\Delta t_{\text{sp}}^0 = \frac{1}{m_{\text{sp}}^0} = \frac{M_{pl}/(\sqrt{6}\xi)}{\dot{\phi}_1} \sim \frac{1}{\sqrt{3}\lambda_H M_{pl}}, \quad (80)$$

which is quite small compared with the naive cutoff time scale $(M_{pl}/\xi)^{-1}$. In Fig. 9, we show our numerical calculations where blue (orange) lines correspond to ϕ_1 (χ) and $x := M_\chi t/\pi$.

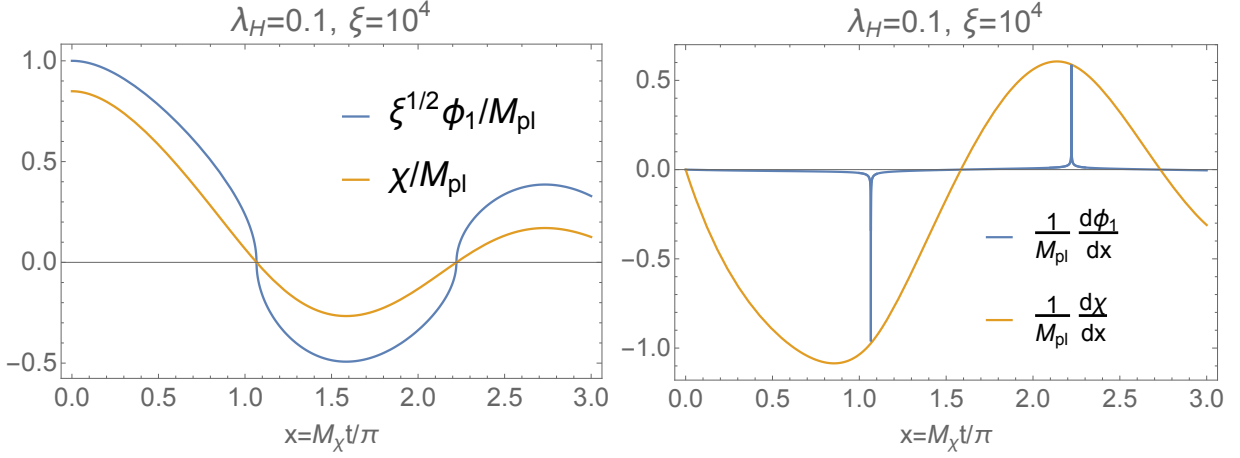


Figure 9: Left: Time evolution of ϕ_1 (blue) and χ (orange). Right: Corresponding time evolution of $\dot{\phi}_1$ (blue) and $\dot{\chi}$ (orange). We can see the spike-like behavior of $\dot{\phi}_1$ around the first zero-crossing.

In the left (right) panel, we show ϕ_1 ($\dot{\phi}_1$). One can in fact see that $\dot{\phi}_1$ shows a spike-like behavior around the first zero crossing and its peak value is consistent with Eq.(79). This behavior of $\dot{\phi}_1(t)$ was first pointed out in [20], and this property plays an important role in particle production after inflation when the mass of the particles depends on the derivatives of ϕ_1 .

For completeness, we present the equation of motion of ϕ_1 . This can be obtained by rewriting Eq. (76) using Eq. (75);

$$\ddot{\phi}_1 + 3\mathcal{H}\dot{\phi}_1 + \frac{d^2\chi}{d\phi_1^2} \frac{d\phi_1}{d\chi} \dot{\phi}_1^2 + \left(\frac{d\phi_1}{d\chi}\right)^2 \frac{\partial V}{\partial \phi_1} = 0. \quad (81)$$

From the above equation of motion and Eq. (79), one can see

$$\frac{d^{2n}\phi_1}{dt^{2n}} \sim \left(\sqrt{\lambda_H} M_{pl}\right)^{2n} \phi_1, \quad \frac{d^{2n+1}\phi_1}{dt^{2n+1}} \sim \left(\sqrt{\lambda_H} M_{pl}\right)^{2n+1} \frac{M_{pl}}{\xi}, \quad \text{for } 0 \leq n \in \mathbb{Z}, \quad (82)$$

for the first zero-crossing. Here we have neglected the Hubble friction term.

Appendix C NG Mode

Here, we present the derivation of the equation for the NG mode. Assuming the Friedmann metric, the kinetic term of θ_J becomes

$$\frac{1}{2} \int d\eta d^3x F^2 \left(\theta_J'^2 - (\nabla\theta_J)^2 \right) = \frac{1}{2} \int d\eta d^3x \left(\theta'^2 - (\nabla\theta)^2 + \frac{F''}{F} \theta^2 \right), \quad (83)$$

where

$$F := \frac{ar_J}{\Omega M_{pl}} \sqrt{1 + \frac{c\Omega^2 \dot{r}_J^2}{\Lambda_J^4}}, \quad \theta := F\theta_J. \quad (84)$$

The frequency ω_k is given by Eq. (48). The background r_J is determined by

$$\ddot{r}_J \left[1 + \frac{3c}{\Lambda_J^4} \dot{r}_J^2 \left(\frac{dr_J}{dr} \right)^2 \right] + 3\mathcal{H}\dot{r}_J \left[1 + \frac{c}{\Lambda_J^4} \dot{r}_J^2 \left(\frac{dr_J}{dr} \right)^2 \right] + \frac{d^2 r}{dr_J^2} \frac{dr_J}{dr} \dot{r}_J^2 - 3 \left(\frac{dr_J}{dr} \right)^2 \frac{c \frac{\partial \Lambda_J}{\partial r_J}}{\Lambda_J^5} \dot{r}_J^4 + \left(\frac{dr_J}{dr} \right)^2 \frac{\partial V}{\partial r_J} = 0, \quad (85)$$

where

$$\frac{dr}{dr_J} = \frac{\sqrt{1 + \xi(1 + 6\xi) \frac{r_J^2}{M_{pl}^2}}}{1 + \frac{\xi r_J^2}{M_{pl}^2}}. \quad (86)$$

References

- [1] F. L. Bezrukov and M. Shaposhnikov, “The Standard Model Higgs boson as the inflaton,” *Phys. Lett. B* **659** (2008) 703–706, [arXiv:0710.3755 \[hep-th\]](#).
- [2] J. Rubio, “Higgs inflation,” *Front. Astron. Space Sci.* **5** (2019) 50, [arXiv:1807.02376 \[hep-ph\]](#).
- [3] C. Steinwachs, A. Barvinsky, A. Kamenshchik, C. Kiefer, and A. Starobinsky, “The Higgs field as an inflaton,” in *12th Marcel Grossmann Meeting on General Relativity*, pp. 1244–1246. 7, 2009.
- [4] G. Isidori, V. S. Rychkov, A. Strumia, and N. Tetradis, “Gravitational corrections to standard model vacuum decay,” *Phys. Rev. D* **77** (2008) 025034, [arXiv:0712.0242 \[hep-ph\]](#).
- [5] Y. Hamada, H. Kawai, and K.-y. Oda, “Minimal Higgs inflation,” *PTEP* **2014** (2014) 023B02, [arXiv:1308.6651 \[hep-ph\]](#).
- [6] M. Fairbairn, P. Grothaus, and R. Hogan, “The Problem with False Vacuum Higgs Inflation,” *JCAP* **06** (2014) 039, [arXiv:1403.7483 \[hep-ph\]](#).
- [7] J. M. Ezquiaga, J. Garcia-Bellido, and E. Ruiz Morales, “Primordial Black Hole production in Critical Higgs Inflation,” *Phys. Lett. B* **776** (2018) 345–349, [arXiv:1705.04861 \[astro-ph.CO\]](#).
- [8] F. Bezrukov, M. Pauly, and J. Rubio, “On the robustness of the primordial power spectrum in renormalized Higgs inflation,” *JCAP* **02** (2018) 040, [arXiv:1706.05007 \[hep-ph\]](#).

- [9] S. Pi, Y.-l. Zhang, Q.-G. Huang, and M. Sasaki, “Scalaron from R^2 -gravity as a heavy field,” *JCAP* **05** (2018) 042, [arXiv:1712.09896 \[astro-ph.CO\]](#).
- [10] S. Rasanen and E. Tomberg, “Planck scale black hole dark matter from Higgs inflation,” *JCAP* **01** (2019) 038, [arXiv:1810.12608 \[astro-ph.CO\]](#).
- [11] D. Y. Cheong, S. M. Lee, and S. C. Park, “Primordial Black Holes in Higgs- R^2 Inflation as a Whole Dark Matter,” [arXiv:1912.12032 \[hep-ph\]](#).
- [12] C. Burgess, H. M. Lee, and M. Trott, “Power-counting and the Validity of the Classical Approximation During Inflation,” *JHEP* **09** (2009) 103, [arXiv:0902.4465 \[hep-ph\]](#).
- [13] J. Barbon and J. Espinosa, “On the Naturalness of Higgs Inflation,” *Phys. Rev. D* **79** (2009) 081302, [arXiv:0903.0355 \[hep-ph\]](#).
- [14] A. Barvinsky, A. Kamenshchik, C. Kiefer, A. Starobinsky, and C. Steinwachs, “Higgs boson, renormalization group, and naturalness in cosmology,” *Eur. Phys. J. C* **72** (2012) 2219, [arXiv:0910.1041 \[hep-ph\]](#).
- [15] C. Burgess, H. M. Lee, and M. Trott, “Comment on Higgs Inflation and Naturalness,” *JHEP* **07** (2010) 007, [arXiv:1002.2730 \[hep-ph\]](#).
- [16] F. Bezrukov, A. Magnin, M. Shaposhnikov, and S. Sibiryakov, “Higgs inflation: consistency and generalisations,” *JHEP* **01** (2011) 016, [arXiv:1008.5157 \[hep-ph\]](#).
- [17] G. F. Giudice and H. M. Lee, “Unitarizing Higgs Inflation,” *Phys. Lett. B* **694** (2011) 294–300, [arXiv:1010.1417 \[hep-ph\]](#).
- [18] J. Rubio and E. S. Tomberg, “Preheating in Palatini Higgs inflation,” *JCAP* **04** (2019) 021, [arXiv:1902.10148 \[hep-ph\]](#).
- [19] A. Karam, M. Raidal, and E. Tomberg, “Gravitational dark matter production in Palatini preheating,” [arXiv:2007.03484 \[astro-ph.CO\]](#).
- [20] Y. Ema, R. Jinno, K. Mukaida, and K. Nakayama, “Violent Preheating in Inflation with Nonminimal Coupling,” *JCAP* **02** (2017) 045, [arXiv:1609.05209 \[hep-ph\]](#).
- [21] M. P. DeCross, D. I. Kaiser, A. Prabhu, C. Prescod-Weinstein, and E. I. Sfakianakis, “Preheating after Multifield Inflation with Nonminimal Couplings, I: Covariant Formalism and Attractor Behavior,” *Phys. Rev. D* **97** no. 2, (2018) 023526, [arXiv:1510.08553 \[astro-ph.CO\]](#).
- [22] M. P. DeCross, D. I. Kaiser, A. Prabhu, C. Prescod-Weinstein, and E. I. Sfakianakis, “Preheating after multifield inflation with nonminimal couplings, II: Resonance Structure,” *Phys. Rev. D* **97** no. 2, (2018) 023527, [arXiv:1610.08868 \[astro-ph.CO\]](#).
- [23] M. P. DeCross, D. I. Kaiser, A. Prabhu, C. Prescod-Weinstein, and E. I. Sfakianakis, “Preheating after multifield inflation with nonminimal couplings, III: Dynamical spacetime results,” *Phys. Rev. D* **97** no. 2, (2018) 023528, [arXiv:1610.08916 \[astro-ph.CO\]](#).

- [24] E. I. Sfakianakis and J. van de Vis, “Preheating after Higgs Inflation: Self-Resonance and Gauge boson production,” *Phys. Rev. D* **99** no. 8, (2019) 083519, [arXiv:1810.01304 \[hep-ph\]](#).
- [25] F. Bezrukov, D. Gorbunov, and M. Shaposhnikov, “On initial conditions for the Hot Big Bang,” *JCAP* **06** (2009) 029, [arXiv:0812.3622 \[hep-ph\]](#).
- [26] J. Garcia-Bellido, D. G. Figueroa, and J. Rubio, “Preheating in the Standard Model with the Higgs-Inflaton coupled to gravity,” *Phys. Rev. D* **79** (2009) 063531, [arXiv:0812.4624 \[hep-ph\]](#).
- [27] Y. Hamada, H. Kawai, Y. Nakanishi, and K.-y. Oda, “Meaning of the field dependence of the renormalization scale in Higgs inflation,” *Phys. Rev. D* **95** no. 10, (2017) 103524, [arXiv:1610.05885 \[hep-th\]](#).
- [28] **Planck** Collaboration, Y. Akrami *et al.*, “Planck 2018 results. X. Constraints on inflation,” *Astron. Astrophys.* **641** (2020) A10, [arXiv:1807.06211 \[astro-ph.CO\]](#).
- [29] G. Degrassi, S. Di Vita, J. Elias-Miro, J. R. Espinosa, G. F. Giudice, G. Isidori, and A. Strumia, “Higgs mass and vacuum stability in the Standard Model at NNLO,” *JHEP* **08** (2012) 098, [arXiv:1205.6497 \[hep-ph\]](#).
- [30] Y. Hamada, H. Kawai, and K.-y. Oda, “Bare Higgs mass at Planck scale,” *Phys. Rev. D* **87** no. 5, (2013) 053009, [arXiv:1210.2538 \[hep-ph\]](#). [Erratum: *Phys.Rev.D* 89, 059901 (2014)].
- [31] D. Buttazzo, G. Degrassi, P. P. Giardino, G. F. Giudice, F. Sala, A. Salvio, and A. Strumia, “Investigating the near-criticality of the Higgs boson,” *JHEP* **12** (2013) 089, [arXiv:1307.3536 \[hep-ph\]](#).
- [32] C. Froggatt and H. B. Nielsen, “Standard model criticality prediction: Top mass 173 +- 5-GeV and Higgs mass 135 +- 9-GeV,” *Phys. Lett. B* **368** (1996) 96–102, [arXiv:hep-ph/9511371](#).
- [33] M. Shaposhnikov and C. Wetterich, “Asymptotic safety of gravity and the Higgs boson mass,” *Phys. Lett. B* **683** (2010) 196–200, [arXiv:0912.0208 \[hep-th\]](#).
- [34] Y. Hamada, H. Kawai, and K. Kawana, “Natural solution to the naturalness problem: The universe does fine-tuning,” *PTEP* **2015** no. 12, (2015) 123B03, [arXiv:1509.05955 \[hep-th\]](#).
- [35] A. Eichhorn, Y. Hamada, J. Lumma, and M. Yamada, “Quantum gravity fluctuations flatten the Planck-scale Higgs potential,” *Phys. Rev. D* **97** no. 8, (2018) 086004, [arXiv:1712.00319 \[hep-th\]](#).
- [36] Y. Hamada, H. Kawai, K.-y. Oda, and S. C. Park, “Higgs Inflation is Still Alive after the Results from BICEP2,” *Phys. Rev. Lett.* **112** no. 24, (2014) 241301, [arXiv:1403.5043 \[hep-ph\]](#).

- [37] F. Bezrukov and M. Shaposhnikov, “Higgs inflation at the critical point,” *Phys. Lett. B* **734** (2014) 249–254, [arXiv:1403.6078 \[hep-ph\]](#).
- [38] Y. Hamada, H. Kawai, K.-y. Oda, and S. C. Park, “Higgs inflation from Standard Model criticality,” *Phys. Rev. D* **91** (2015) 053008, [arXiv:1408.4864 \[hep-ph\]](#).
- [39] A. Adams, N. Arkani-Hamed, S. Dubovsky, A. Nicolis, and R. Rattazzi, “Causality, analyticity and an IR obstruction to UV completion,” *JHEP* **10** (2006) 014, [arXiv:hep-th/0602178](#).
- [40] L. Kofman, A. D. Linde, and A. A. Starobinsky, “Reheating after inflation,” *Phys. Rev. Lett.* **73** (1994) 3195–3198, [arXiv:hep-th/9405187](#).
- [41] L. Kofman, A. D. Linde, and A. A. Starobinsky, “Towards the theory of reheating after inflation,” *Phys. Rev. D* **56** (1997) 3258–3295, [arXiv:hep-ph/9704452](#).
- [42] K. D. Lozanov and M. A. Amin, “The charged inflaton and its gauge fields: preheating and initial conditions for reheating,” *JCAP* **06** (2016) 032, [arXiv:1603.05663 \[hep-ph\]](#).
- [43] R. Nguyen, J. van de Vis, E. I. Sfakianakis, J. T. Giblin, and D. I. Kaiser, “Nonlinear Dynamics of Preheating after Multifield Inflation with Nonminimal Couplings,” *Phys. Rev. Lett.* **123** no. 17, (2019) 171301, [arXiv:1905.12562 \[hep-ph\]](#).